ARTICLE
Journal of Cellular Biochemistry 113:1754–1765 (2012)

Journal of Cellular Biochemistry

Odontogenic Ameloblasts-Associated Protein (ODAM), via Phosphorylation by Bone Morphogenetic Protein Receptor Type IB (BMPR–IB), Is Implicated in Ameloblast Differentiation

Hye-Kyung Lee,[1] Jong-Tae Park,[2] Young-Sik Cho,[3] Hyun-Sook Bae,[3] Moon-Il Cho,[4] and Joo-Cheol Park[1*]

[1] *Department of Oral Histology-Developmental Biology, School of Dentistry and Dental Research Institute, BK 21, Seoul National University, Seoul 110-749, Korea*

[2] *Division in Anatomy and Developmental Biology, Department of Oral Biology, BK 21, College of Dentistry, Yonsei University, Seoul 120-752, Korea*

[3] *Department of Dental Hygiene, Namseoul University, Cheon-An 331-707, Korea*

[4] *Department of Oral Biology, School of Dental Medicine, State University of New York at Buffalo, NY 14214-3092*

ABSTRACT

To elucidate the function of the odontogenic ameloblast-associated protein (ODAM) in ameloblasts, we identified more than 74 proteins that interact with ODAM using protoarray. Of the identified proteins, bone morphogenetic protein receptor type-IB (BMPR-IB) was physiologically relevant in differentiating ameloblasts. ODAM and BMPR-IB exhibited similar patterns of expression in vitro, during ameloblast differentiation. ODAM and BMPR-IB interacted through the C-terminus of ODAM, which resulted in increased ODAM phosphorylation in the presence of bone morphogenetic protein 2 (BMP-2). Immunoprecipitation assays using Ser-Xaa-Glu (SXE) mutants of ODAM demonstrated that the phosphorylation of ODAM by BMPR-IB occurs at this motif, and this phosphorylation is required for the activation of MAPKs. ODAM phosphorylation was detected in ameloblasts during ameloblast differentiation and enamel mineralization in vitro and involved in the activation of downstream factors of MAPKs. Therefore, the BMP-2-BMPR-IB-ODAM-MAPK signaling cascade has important roles in ameloblast differentiation and enamel mineralization. Our data suggest that ODAM facilitates the progression of tooth development in cooperation with BMPR-IB through distinct domains of ODAM. J. Cell. Biochem. 113: 1754–1765, 2012.

KEY WORDS: ODAM; BMPR-IB; MAPK; AMELOBLAST; DIFFERENTIATION

The odontogenic ameloblast-associated protein (ODAM) has been implicated in diverse activities such as ameloblast differentiation, enamel maturation, formation and regeneration of the junctional epithelium (JE), and tumor growth and metastasis [Moffatt et al., 2008; Lee et al., 2010; Kestler et al., 2011]. ODAM localizes to the nucleus, cytoplasm, and extracellular matrix of differentiating ameloblasts. Nuclear ODAM was found to serve as an important regulator of enamel mineralization through the regulation of MMP-20 [Lee et al., 2010]. ODAM is also expressed in the reducing enamel organ and JE [Nishio et al., 2010a]. The expression of ODAM by epithelial cell rests of Malassez (ERM) at an early timepoint following the disruption of periodontal integrity suggests that this protein may be involved in the initial events of periodontal healing and regeneration [Nishio et al., 2010b]. In addition, although the biological function of ODAM has not been established, it also appears to serve as a novel and favorable prognostic biomarker of malignancy, as demonstrated by the statistically significant correlation between the nuclear presence of ODAM and improved 5-year survival rates among breast cancer patients, irrespective of disease stage [Kestler et al., 2011]. Despite their presence in various cells and tissues that implies for multiple regulatory functions, the function of cytoplasmic and extracellular ODAM in secretory- or maturation-stage ameloblasts, JE, and various cancer cells has not yet been determined.

Grant sponsor: Ministry for Health, Welfare, and Family Affairs, Republic of Korea; Grant number: 1020140.
*Correspondence to: Joo-Cheol Park, Department of Oral Histology-Developmental Biology, School of Dentistry, Seoul National University, 28, Yeongun-Dong, Chongro-Gu, Seoul 110-749, Korea. E-mail: jcapark@snu.ac.kr
Received 19 December 2011; Accepted 21 December 2011 • DOI 10.1002/jcb.24047 •
Published online 28 December 2011 in Wiley Online Library (wileyonlinelibrary.com).

During tooth development, specific epithelial–mesenchymal interactions control odontogenesis, which consists of highly organized differentiation programs such as tooth initiation, morphogenesis, epithelial histogenesis, and cytodifferentiation [Nadiri et al., 2006]. These interactions are regulated by several signaling molecules, including bone morphogenetic proteins (BMPs) and transforming growth factor-beta (TGF-β) that are involved in cell differentiation and matrix protein production [Moriguchi et al., 2010]. BMPs transduce their signals by binding to different type I and type II serine/threonine kinase membrane receptors and inducing their dimerization. Three type I BMP receptors (BMPR-IA, BMPR-IB, and ActR-I), and two type II receptors (BMPR-II and ActR-II) have been identified. The effects of BMPs on cell proliferation are mediated by BMPR-IA, while the stimulation of cell differentiation by BMPs is mediated by BMPR-IB in several different models such as neural precursor cells, osteoblasts, and chondrocytes [Onishi et al., 1998; Panchision et al., 2001].

The cytokines BMP-2 and BMP-4 and their receptors have been reported to induce the differentiation of precursor cells into ameloblasts and odontoblasts, which participate in enamel and dentin formation [Aberg et al., 1997; Coin et al., 1999; Nadiri et al., 2006]. The BMP-2 gene was markedly upregulated in ameloblasts at the maturation stage compared with its expression in other stages [Yamamoto et al., 2006]. In addition, the changes in the pattern of expression of BMP receptors may control the specification of BMP signaling at different stages of tooth development [Nadiri et al., 2006]. Recent studies also demonstrated that BMP and BMPR-1B are localized in the epithelial sheath [Kemoun et al., 2007] and that they regulate sheath development [Hosoya et al., 2008]. However, the function and molecular mechanisms of the activities of BMP-2 and BMPR-IB in ameloblasts during enamel development have not yet been clarified.

Earlier studies suggested a role for ODAM and the importance of its signaling pathway in ameloblast differentiation and maturation [Moffatt et al., 2008; Lee et al., 2010]. The objective of this study was to examine ODAM-interacting proteins and their physiological roles during amelogenesis. In the present study, we identified ODAM-interacting proteins by using protoarray screening and found a protein with functional importance in amelogenesis. The signaling pathway, BMPR-IB-mediated ODAM phosphorylation, and its functional implications during amelogenesis were also examined.

MATERIALS AND METHODS

PROTEIN MICROARRAY

A Protoarray kit (Version 3.0, Invitrogen, Carlsbad, CA) was used for the protein microarray screening experiments. After blocking the array in blocking buffer (PBS, 1% BSA, 0.1% Tween 20) for 1 h at 4°C, 10 μg aliquots of biotinylated ODAM or GST control diluted in 120 μl of probing buffer (PBS containing 0.5 mM DTT, 5 mM $MgCl_2$, 5% glycerol, 0.05% Triton X-100, and Calbiochem protease inhibitor cocktail) were added to the array, which was incubated at 4°C for an additional 90 min. The arrays were then washed three times in ice cold probing buffer prior to the addition of streptavidin–alkaline phosphatase (Invitrogen) diluted in probing buffer to a final concentration of 0.25 μg/ml. Arrays were incubated for 30 min on ice, washed three times in probing buffer and then dried for 2 h. After slides were washed, 30 ml of a streptavidin-conjugated Alexa Fluor® 647 antibody solution (Invitrogen) were added immediately, and the slides were incubated at 4–6°C for 30 min. After washing, the hybridized slides were scanned with GenePix 4000B (Axon Instruments, Redwood City, CA) at 635 nm with a PMT gain of 600 (a laser power of 100% and a focus point of 10 μm). Arrays were imaged using the software program GenePix Pro 6.0 (Axon Instruments), and the images were exported to a Microsoft Excel file and analyzed using Invitrogen Prospector version 4.0 (Invitrogen) using the default settings. Significant interactions were identified on the basis of a *Z*-score cutoff value of 3.0 with the values obtained from the biotin-GST experiment being subtracted from the corresponding values of the biotin-ODAM experiment.

CELL LINES AND CELL CULTURE

Immortalized ameloblast-lineage cells (ALCs), an ameloblastic cell line derived from the tooth germs of newborn C57/Bl6J mouse lower molars, were kindly provided by Dr T. Sugiyama (Akita University School of Medicine, Akita, Japan). ALCs were cultured in minimum essential medium (MEM) supplemented with 5% heat inactivated fetal bovine serum (FBS), 10 ng/ml of the recombinant human epithelial growth factor (EGF; Sigma–Aldrich, Gillingham, UK), and antibiotic-antimycotic (Invitrogen) in a 5% CO_2 atmosphere at 37°C. HEK 293 cells were cultured in Dulbecco's modified Eagle's medium (DMEM) supplemented with 10% heat inactivated FBS and antibiotic–antimycotic (Invitrogen) in a 5% CO_2 atmosphere at 37°C.

PLASMIDS AND CLONING

ODAM mutants were constructed using standard methods and verified by sequencing. The cDNAs of the ODAM deletion mutants were amplified by PCR and subcloned into Flag-tagged pcDNA3 (Invitrogen). Other ODAM mutants with point mutations or deletion of the Ser-Baa-Glu (SXE; Xaa represents any amino acid) motif (amino acids 29–31) were created by recombinant PCR and subcloned into the Flag-pcDNA3 vector (Invitrogen). A GFP-tagged construct was created in pEGFP-C3 (BD Biosciences, Palo Alto, CA). Based on the 19-nucleotide ODAM siRNA sequence (5′-AAGTGCCT-CAAGATCAAAC-3′) selected using the siRNA Target Finder and Design Tool (Ambion, Austin, TX), a plasmid expressing ODAM siRNA was prepared using the pSilencer 1.0-U6 siRNA expression vector (Ambion) according to the manufacturer's instructions. HA-tagged wild type, constitutively active (QD), and dominant-negative (KR) BMPR-IB vectors were constructed using pcDNA3 vectors obtained from Hyun-Mo Ryoo (Seoul National University, Seoul, Korea).

RNA INTERFERENCE

The sequences of the custom siRNA duplex (Stealth System, Invitrogen) were as follows: for BMPR-IB, sense, 5′-AGAUAUU-GUUGACUGAGUCUUCCGG-3′ and antisense, 5′-CCGGAACACU-CAGUCAACAAUAUCU-3′. The siRNA duplex control used was the Stealth RNAi negative control with medium GC content (Invitrogen). Transfection of siRNA was performed with Metafectene PRO reagent

(Biontex, Bavaria, Germany) in HEK 293 or ALC cells according to the manufacturer's instructions. Knockdown of BMPR-IB was verified by western blotting.

WESTERN BLOT ANALYSIS

Proteins were extracted from cell lysates after lysis in Nonidet P-40 (NP-40) lysis buffer (50 mM Tris–Cl, pH 7.4, 150 mM NaCl, 1% NP-40, 2 mM EDTA, pH 7.4, and protease inhibitor). Samples were separated on denaturing 10–12% Tris–HCl polyacrylamide gels and transferred to nitrocellulose membranes. The membranes were blocked for 1 h with 5% nonfat dry milk in PBS containing 0.1% Tween 20 (PBS-T), washed with PBS-T, and incubated for 16 h with primary antibody diluted in PBS-T buffer (1:1,000) at 4°C. Rabbit and affinity-purified polyclonal anti-ODAM antibodies were generated against amino acids residues 102–114 or 241–251 of ODAM. Other commercially available primary antibodies used were mouse monoclonal anti-HA antibody (E10176EF; Covance, Emeryville, CA), mouse monoclonal anti-Flag M2 antibody (F-3165; Sigma–Aldrich), rabbit polyclonal BMPR-IB antibody (sc-25455; Santa Cruz Biotechnology, Santa Cruz, CA), rabbit polyclonal anti-p-Ser/Thr antibody (#9381; Cell Signaling, Danvers, MA), rabbit polyclonal anti-p-ERK antibody (#9101; Cell Signaling), rabbit polyclonal anti-p-p38 antibody (#4631; Cell Signaling), rabbit polyclonal p-JNK antibody (#9251; Cell Signaling), rabbit polyclonal p-paxillin antibody (#2541; Cell Signaling), rabbit polyclonal Hsp27 antibody (#2442; Cell Signaling), goat polyclonal lamin B antibody (sc-6216; Santa Cruz) and rabbit anti-GAPDH IgG (sc-25778; Santa Cruz). After washing, the membranes were then incubated with horseradish peroxidase-conjugated goat anti-mouse (sc-2031; Santa Cruz), goat anti-rabbit-IgG (sc-2004; Santa Cruz), and rabbit anti-goat-IgG (sc-2768; Santa Cruz) for 1 h. Labeled protein bands were detected using an enhanced chemiluminescence system (Dogen, Cambridge, MA) on autoradiograph films.

IMMUNOFLUORESCENCE

To locate endogenous ODAM and BMPR-IB, ALC cells were washed with PBS, fixed with 4% paraformaldehyde in PBS for 10 min at room temperature, and then permeabilized for 5 min in PBS containing 0.5% Triton X-100. After washing, cells were incubated with anti-ODAM antibody or anti-BMPR-IB (1:200 dilution) in blocking buffer (PBS and 2% BSA) for 2 h and then incubated with FITC-conjugated anti-rabbit IgG (1:200 dilution; Amersham Pharmacia Biotech, Piscataway, NJ). Cells were transfected with GFP-ODAM or HA-BMPR-IB to locate overexpressed ODAM and BMPR-IB. Endogenous or exogenous colocalization of BMPR-IB was determined by staining the protein with rabbit polyclonal anti-BMPR-IB antibody and Texas Red-conjugated anti-rabbit IgG in ALC cells. After the washing step, the cells were visualized under a fluorescence microscope (AX70; Olympus Optical Co, Tokyo, Japan). Chromosomal DNA in the nucleus was stained using DAPI.

COIMMUNOPRECIPITATION (CO-IP) ASSAY

After transfection with the indicated plasmid DNA using Metafectene PRO reagent (Biontex), HEK 293 or ALC cells were washed in PBS, and cell lysates were prepared by adding 1 ml of RIPA buffer (50 mM Tris–Cl [pH 7.5], 150 mM NaCl, 1% Nonidet P-40, 1 mM EDTA, 1 mM PMSF, 1 mM Na_3VO_4, and 1 mM NaF) supplemented with protease inhibitors (Roche Molecular Biochemicals, Mannheim, Germany). Lysates were incubated at 4°C for 2 h with a 1:200 dilution of the indicated antibody: mouse monoclonal anti-Flag, anti-HA, or anti-ODAM. After 2 h of incubation at 4°C with A/G-agarose beads (Santa Cruz), the beads were washed three times with RIPA buffer and the immune complexes were released from the beads by boiling. Following electrophoresis on 10% SDS–polyacrylamide gels, immunoprecipitates were analyzed by Western blotting using either anti-HA antibody, anti-BMPR-IB antibody, or anti-p-Ser/Thr antibody.

IN VITRO KINASE ASSAY

For in vitro kinase assays, the indicated ODAM and BMPR-IB constructs were in vitro translated in the TNT reticulocyte system (Promega, Madison, WI) and approximately equal amounts of translated ODAM and BMPR-IB proteins were mixed in kinase buffer (20 mM HEPES, pH 7.5, 20 mM $MgCl_2$, 1 mM EDTA, 2 mM NaF, 2 mM glycerophosphate, 1 mM DTT, 10 mM ATP). The substrates were precipitated using anti-Flag antibody and A/G-agarose beads overnight at 4°C. The phosphorylated proteins were visualized by Western blotting using anti-Flag antibody instead of autoradiography.

ALIZARIN RED S STAINING

To induce cell differentiation and mineralized nodule formation, confluent ALC cells were treated with 50 μg/ml ascorbic acid and 10 mmol/L β-glycerolphosphate, for up to 2 weeks. Cells were fixed with 70% ethanol for 20 min and stained with 1% alizarin red S (Sigma–Aldrich) in 0.1% NH_4OH at pH 4.2–4.4. Mineralization assays were performed using staining with alizarin red S solution. The cells were evaluated on days 0, 4, 7, 10, and 14. The stained cells were collected by centrifugation at 13,000 rpm for 10 min at 4°C. Cell lysates were solubilized with 0.5 ml of 5% SDS in 0.5 N HCl for 30 min at room temperature (vortexing or pipetting). Solubilized stain (0.1 ml) was transferred to the wells of a 96-well plate, and absorbance was measured at 405 nm.

ALKALINE PHOSPHATASE (ALP) STAINING

To detect ALP activity, ALCs and the stable cell colonies were washed in PBS three times, fixed with 3.7% formaldehyde in PBS for 10 min, washed in distilled water three times, and then stained with a Fast Blue RR Salt capsule and naphthol AS-MX Phosphate Alkaline Solution (Sigma). Then, Tris–HCl buffer (0.1 M, pH 8.2, 7.8 ml) containing naphthol AS-BI phosphate (Sigma, 2 mg), dimethyl formamide (Sigma, 200 μl), 0.1 M levamisole (Sigma, 1 ml), and fast red violet (Sigma, 10 mg) were added, and the cells were incubated for 15 min in shaded conditions.

STATISTICAL ANALYSIS

The data were analyzed for statistical significance using a non parametric Mann–Whitney test.

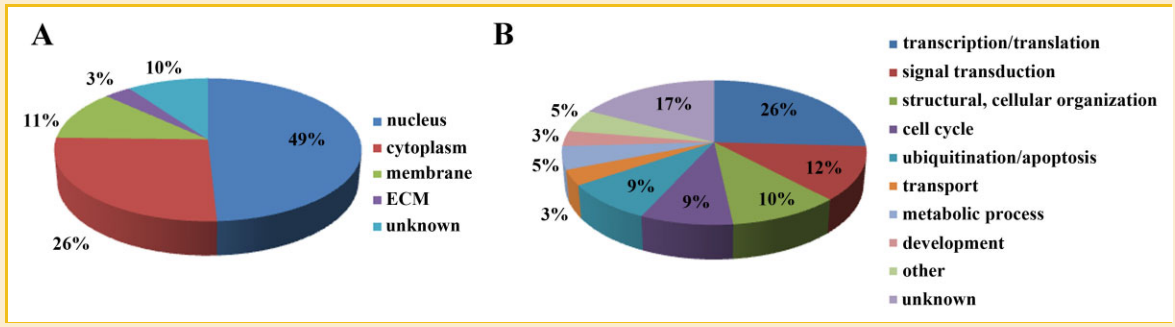

Fig. 1. Summary of the protoarray analysis. Cellular localization (A) and functional classification (B) of the identified proteins that interacted with ODAM. The resulting 74 genes were analyzed using homology-based functional or localization annotation. The values in the pie chart represent the number of functional or localization annotations in each division. [Color figure can be seen in the online version of this article, available at http://wileyonlinelibrary.com/journal/jcb]

RESULTS

SCREENING OF ODAM-INTERACTING PROTEINS USING A PROTOARRAY

Few studies have investigated the function of cytoplasmic or extracellular ODAM in ameloblasts, JE cells, and various cancer cells. The identification of new physiological proteins interacting with ODAM is required to elucidate the biological function of ODAM. To identify ODAM-interacting proteins, we used human protoarray spotted with 37000 GST-tagged human proteins on high-density glass slides.

Consistent with the known subcellular distribution of ODAM, the majority of identified ODAM-interacting proteins localized in the cytoplasm and/or nucleus. The prevalence rates of the overall identified proteins in the nucleus, cytoplasm, and extracellular matrix were 49%, 26%, and 3%, respectively; the values were described as proportional Venn diagram (Fig. 1A). Six proteins were expressed simultaneously in the nucleus and cytoplasm (data not shown). An ontological analysis revealed that proteins related to transcription/translation formed the largest category, comprising 26% of the interactome, whereas 12% and 10% of interacting proteins are involved in signal transduction and structural/cellular organization, respectively (Fig. 1B).

Among the final list, the majority of the putative ODAM-interacting proteins appeared to be unknown, including MEF2D, aurora kinase A, MLK3, and RET, which had not been previously reported as ODAM-interacting proteins or regulating factors for tooth formation (Table I). Aurora kinase A was previously reported to promote cell proliferation and tumorigenesis [Vader and Lens, 2008]. MLK3 is a serine/threonine and MAPK8/JNK kinase [Liou et al., 2010]. The identified ODAM-interacting kinases such as anaplastic lymphoma kinase 1 and BMPR-IB are related to the BMP signaling pathway [Panchision et al., 2001]. Considering the canonical role of BMPR-IB as a member of the BMP receptor family, this finding is considered a strong validation of specificity and usefulness of the screen.

CORRELATION OF ODAM EXPRESSION WITH BMPR-IB DURING AMELOBLASTS DIFFERENTIATION IN VITRO

BMPR-IB is present in the mesenchyme at the bud stage, in the epithelium at the cap stage, and in ameloblasts and odontoblasts at the late bell stage [Nadiri et al., 2006]. First of all, we determined the subcellular distribution of endogenous ODAM and BMPR-IB in ALC cells to further substantiate their interaction. Confocal microscopy showed that the localization of endogenous or exogenous ODAM was specific in the nucleus and cytoplasm of ameloblasts (Fig. 2A, a, h, and l). In addition, endogenous or exogenous BMPR-IB was localized in the cytoplasm as well as plasma membrane of ameloblasts (Fig. 2A, d, i, and m). GFP-tagged exogenous ODAM and endogenous BMPR-IB were colocalized in the cytoplasm of ameloblasts (Fig. 2A, h–k). Exogenous GFP-tagged ODAM and HA-tagged BMPR-IB were also coexpressed in the cytoplasm of ameloblasts (Fig. 2A, l–o).

TABLE I. The List of Proteins Highly Interacting With ODAM

Database ID	Protein	Localization	Function
NM021639.2	SP192	Nucleus	Transcription factor
BC013966.2	FAM64A	Nucleus	Transcription factor
NM006775.1	KH domain	Nucleus	RNA binding protein
BC054520.1	MEF2D	Nucleus	Transcription factor
BC001280.1	Aurora kinase A	Nucleus	Serine/threonine kinases, cell proliferation
NM013375.2	TBP	Nucleus	TATA box binding, basal transcription
BC053557.1	Zinc finger protein 740	Nucleus	DNA binding motif, transcription regulation
NM003621.1	PPFIBP2	Cytoplasm	Tyrosine phosphatase, adhesion
NM002419.2	MLK3	Cytoplasm	Serine/threonine kinase, MARK/JNK activation
NM003975.1	SH2D2A	Cytoplasm	Tyrosine kinase activation, cell proliferation regulation
NM001203.1	BMPR1B	Cytoplasm	Serine/threonine kinases, development
NM020975.2	RET	ECM	Signal transduction

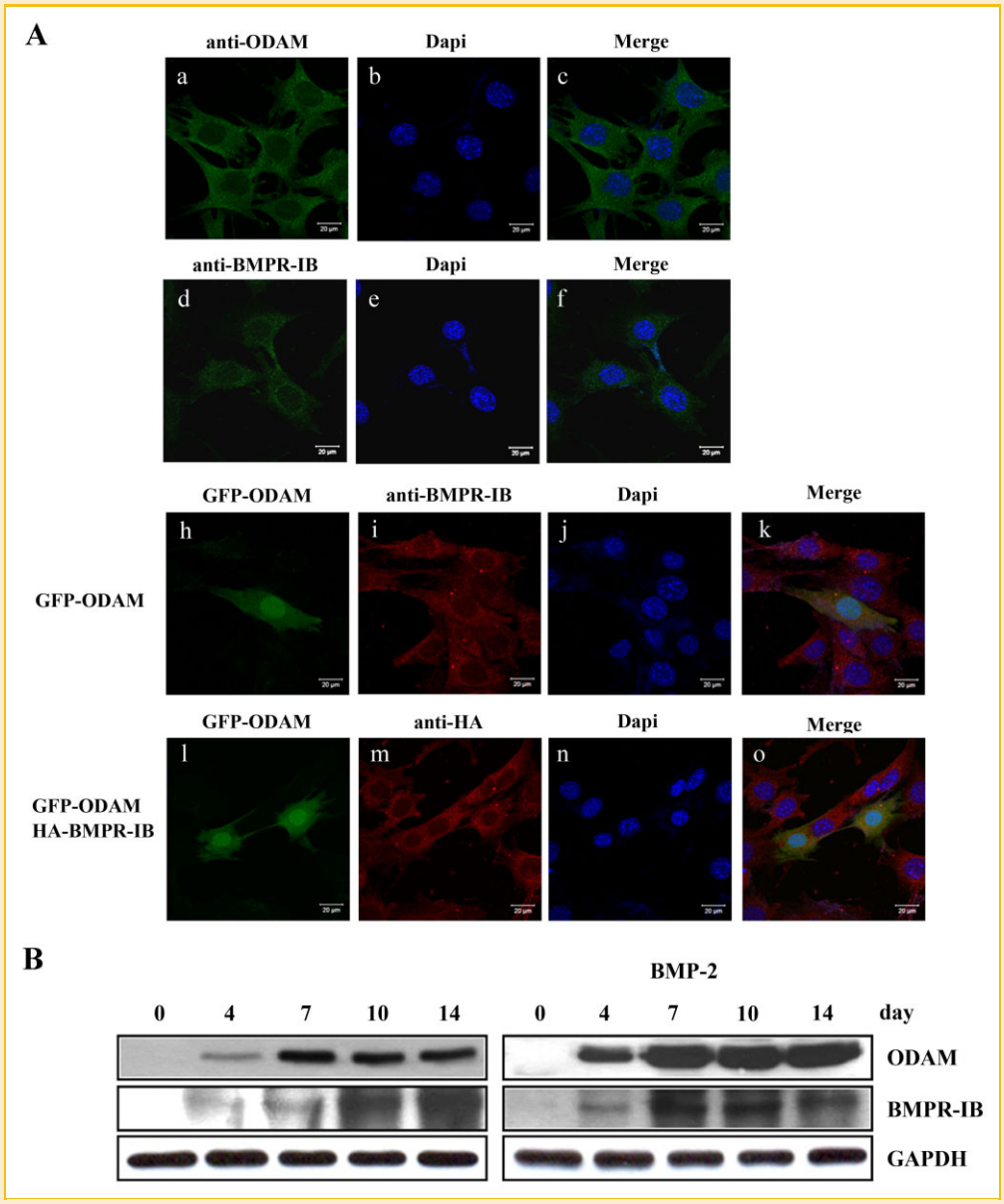

Fig. 2. Expression patterns of ODAM and BMPR-IB during ameloblast differentiation in vitro. A: Localization of ODAM and BMPR-IB in ALC cells was investigated by immunofluorescence. Endogenous ODAM and BMPR-IB were immunostained with anti-ODAM and anti-BMPR-IB antibodies in ALC cells. GFP-tagged ODAM and HA-tagged BMPR-IB constructs were transfected into ALC cells. Exogenous BMPR-IB was immunostained by anti-HA antibody and GFP-ODAM was detected by immunofluorescence. Nuclei were stained with DAPI. Bars = 20 μm. B: ODAM and BMPR-IB expression during ameloblast differentiation in vitro. The expression of ODAM and BMPR-IB during the in vitro differentiation of ALC cells in the presence (right panel) or absence (left panel) of BMP-2 treatment was analyzed by Western blot. GAPDH was used as a control. [Color figure can be seen in the online version of this article, available at http://wileyonlinelibrary.com/journal/jcb]

BMP-2 has important roles in the differentiation of ameloblasts in vitro [Coin et al., 1999]. To gain insight into the expression pattern of ODAM and BMPR-IB during the differentiation of ameloblasts in vitro, ALC cells were grown in differentiation medium for 14 days in the absence or presence of BMP-2. ODAM and BMPR-IB expression increased as ameloblasts differentiation and mineralization progressed of the course of the culture (Fig. 2B, left panel). The addition of BMP-2 increased ODAM and BMPR-IB protein expression compared to that in normal ALC cells (Fig. 2B, right panel). These findings suggest that ODAM and BMPR-IB are functionally related to the differentiation and maturation of ameloblasts in the presence of BMP-2.

BMPR-IB INTERACTS WITH ODAM THROUGH THE C-TERMINAL DOMAIN OF ODAM

To investigate whether ODAM could mutually interact with BMPR-IB as suggested by the protoarray data, a co-IP analysis was performed in ALC cells after transfection of the ODAM expression plasmid. Transfected ODAM co-precipitated with BMPR-IB, but the empty vector alone did not co-precipitate with BMPR-IB (Fig. 3A).

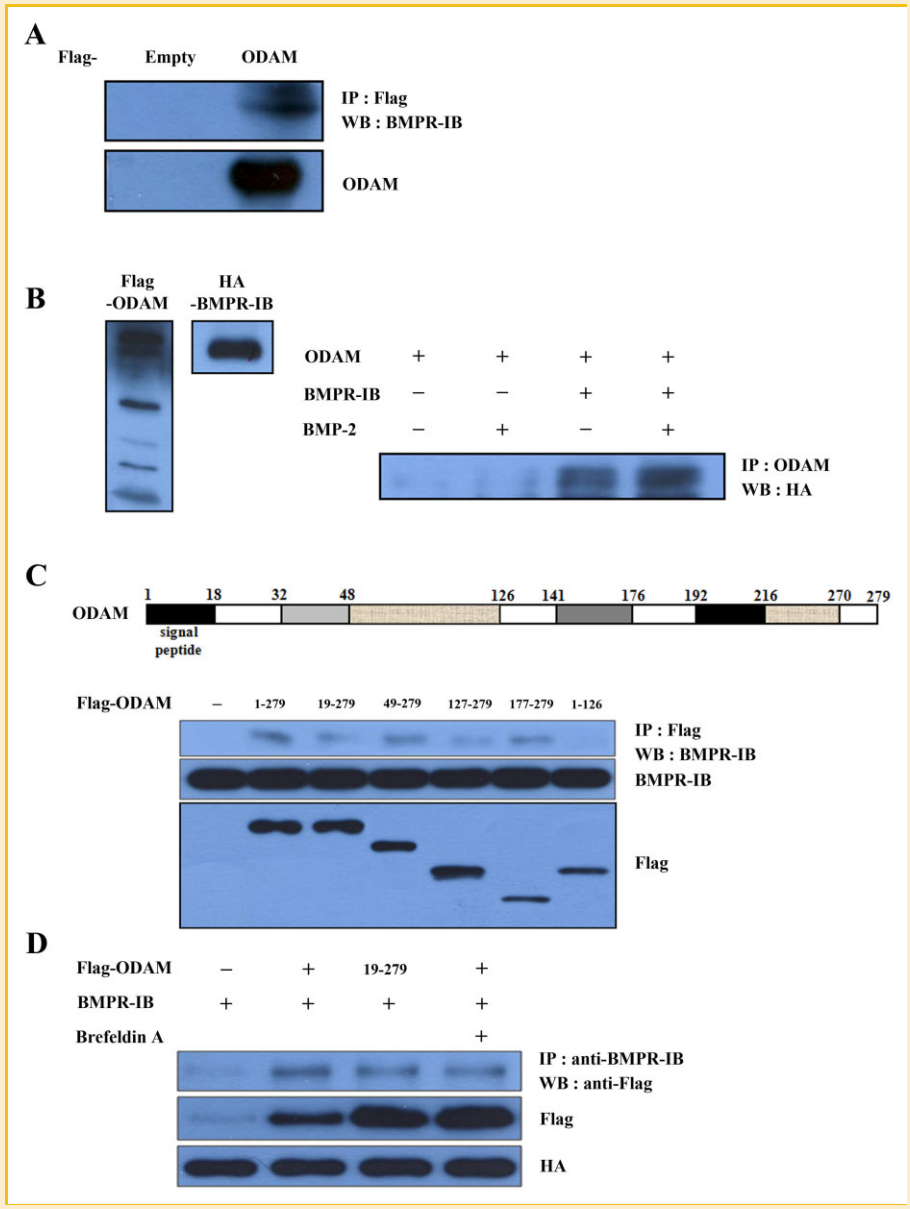

Fig. 3. Interaction between ODAM and BMPR-IB in vitro. A: HEK 293 cells were transfected with Flag-tagged ODAM and treated with BMP-2 (100 ng/ml) for 16 h. Immunoprecipitation was performed using anti-Flag antibody as indicated. Precipitated proteins were visualized by Western blotting using anti-BMPR-IB antibody. B: Direct interaction of ODAM with BMPR-IB. Flag-ODAM and HA-BMPR-IB were translated in vitro by TNT reticulocyte (left panel). In vitro-translated ODAM and BMPR-IB were incubated in the presence of BMP-2. Immunoprecipitation was performed using anti-Flag antibody as indicated. Bound proteins that precipitated with anti-ODAM antibody were visualized by Western blotting. Input was 10% of the labeled sample used in the assay. C: Mapping of the ODAM domain required for its binding with BMPR-IB. HEK 293 cells were transfected with Flag-tagged ODAM or its deletion constructs and treated with BMP-2. Western blotting using anti-BMPR-IB antibody was performed for precipitates obtained using the anti-Flag antibody. D: Confirmation of interaction between ODAM with BMPR-IB in the cytoplasm of ALC cells. ALC cells were transfected with a Flag-tagged ODAM or a signal peptide deletion construct (a.a. 19–279). ODAM secretion was also inhibited by brefeldin A. Immunoprecipitation was performed using anti-BMPR-IB antibody as indicated. Bound proteins that precipitated with anti-Flag antibody were visualized by Western blotting. [Color figure can be seen in the online version of this article, available at http://wileyonlinelibrary.com/journal/jcb]

To investigate the direct interaction between ODAM and BMPR-IB proteins, we performed a specific protein pull-down analysis with in vitro-translated HA-tagged BMPR-IB and Flag-tagged ODAM proteins. ODAM interacted only weakly with BMPR-IB in the absence of BMP-2, but strongly in the presence of BMP-2 (Fig. 3B). This result confirmed the direct in vitro interaction between ODAM and BMPR-IB and suggested that their interaction is involved in the BMP signaling pathway.

To map the ODAM binding domain that was required for its mutual interaction with BMPR-IB, we performed immunoprecipitation experiments using ODAM deletion constructs in pcDNA3-Flag vectors. Immunoprecipitation with Flag antibody followed by cross-

blotting with BMPR-IB antibody demonstrated that deletion of the C-terminal region of ODAM (177–279 amino acids) affected the interaction between ODAM and BMPR-IB (Fig. 3C, 1–126). This result suggests that the C-terminal domain containing 177–279 region of ODAM is necessary for the interaction of ODAM with BMPR-IB.

To confirm the interaction between ODAM and BMPR-IB in the cytoplasm of ameloblasts, ALC cells were transfected with a Flag-ODAM full length construct or a signal peptide deletion mutant of ODAM in the absent or presence of brefeldin A, an inhibitor of protein secretion. The mutant ODAM was expressed in the cytoplasm and nucleus, but not in the culture medium [Lee et al., 2010]. In the present study, IP demonstrated that exogenous ODAM interacted with exogenous BMPR-IB in ameloblasts. In addition, a signal peptide deletion of ODAM construct or brefeldin A treatment hardly influenced the interaction of ODAM and BMPR-IB (Fig. 3D). These findings suggest that ODAM interacts with BMPR-IB through its cytoplasmic domain in the cytoplasm of ameloblasts.

BMPR-IB MEDIATES THE PHOSPHORYLATION OF ODAM

Upon interacting with a ligand, such as BMP-2, the activated kinase domain of BMPR-II phosphorylates BMPR-I, which in turn initiates intracellular signaling through the direct interaction and phosphorylation of a set of BMP-restricted Smad proteins (Smad1/5/8) [Hardwick et al., 2008]. To delineate whether biomechanical signals such as BMP-2 activated ODAM phosphorylation via the activation of BMPR-IB in ameloblasts, immunoprecipitation using anti-Flag antibody and immunoblotted with anti-p-Ser/Thr antibody were performed. ODAM phosphorylation was detected after BMP-2 treatment and ODAM overexpression (Fig. 4A). In the presence of BMP-2 treatment, both ODAM and BMPR-IB overexpression increased the phosphorylation of ODAM significantly (Fig. 4B). However, siRNA-mediated BMPR-IB depletion in ALC cells suppressed the phosphorylation of ODAM (Fig. 4C).

During signal transduction, BMPR-I is activated by phosphorylation of its serine and threonine residues in the GS domain. The activated type I receptor propagates the signals via the subsequent phosphorylation of other protein substrates [Fujii et al., 1999]. For example, within the GS domain, a glutamine-to-aspartate mutation at position 233 constitutively activates the ALK3 receptor. In contrast, a lysine-to-arginine mutation at position 261 generates a kinase-deficient ALK3 receptor. This mutant can bind ligands but cannot transduce signals [Wieser et al., 1995]. Similar to these reports, to determine whether activation of the BMP-signaling components was sufficient to induce ODAM phosphorylation, we established stable cell lines expressing constitutively active BMPR-IB (ALK6 QD), dominant-negative BMPR-IB (ALK6 KR), and wild-type ODAM. Then, for each stably transfected molecules, we selected two representative clones by Western blotting. Constitutively activated BMPR-IB strongly induced ODAM phosphorylation in the presence of BMP-2 treatment. In contrast, forced expression of the dominant-negative BMPR-IB partially or completely blocked ODAM phosphorylation even in the presence of BMP-2 (Fig. 4D). Afterward, we examined whether BMPR-IB could directly induce the phosphorylation of ODAM. In vitro kinase assays were performed using the in vitro-translated HA-BMPR-IB wild-type, QD, and KR vectors with Flag-tagged ODAM. As expected, using ALK6 QD, ODAM was phosphorylated by BMPR-IB irrespective of the presence of BMP-2 (Fig. 4E). This indicates that BMPR-IB mediates the phosphorylation of ODAM induced by BMP-2.

IDENTIFICATION OF ODAM PHOSPHORYLATION SITES BY BMPR-IB

ODAM is classified as part of the secretory calcium-binding phosphoprotein (SCPP) gene cluster on the basis of its genomic location and architecture. This cluster contains a putative phosphorylation site in the SXE motif coded by the 3′-end of exon 3 [Kawasaki and Weiss, 2003]. To elucidate the ODAM domains required for its phosphorylation, Flag-tagged ODAM deletion constructs were generated, and the expression of each construct was monitored using an anti-Flag antibody. Immunoprecipitation assays using Flag-tagged ODAM deletion constructs indicated that the fragments containing the SXE motif (amino acids 29–31) of ODAM could be phosphorylated by BMPR-IB (Fig. 4F). The fragment containing amino acids 1–126 of ODAM was not phosphorylated by BMPR-IB because it did not contain amino acids 177–279 of ODAM, which are necessary for the interaction of ODAM with BMPR-IB.

SCPP family genes such as ODAM and amelotin, the SASNSxELL motif at amino acids 25–33 (exon 3 and beginning of exon 4), is well conserved and is a probable phosphorylation site [Sire et al., 2007]. ODAM is potentially phosphorylated by BMPR-IB at the SXE motif. To examine the induction of ODAM phosphorylation at the N-terminal SXE motif, two mutants of the SXE motif (AXE or ΔSXE) were subsequently generated by PCR and subcloned into pcDNA3. Both of the mutations blocked BMPR-IB-induced ODAM phosphorylation (Fig. 4G). Overall, these data suggest that the N-terminal SXE motif in ODAM is important for the BMP-2-dependent phosphorylation of ODAM by BMPR-IB.

ODAM PHOSPHORYLATION INDUCED BY BMP SIGNALING ACTIVATES THE MAPK PATHWAY IN AMELOBLASTS

Previous data revealed an interaction between ODAM and BMPR-IB and the phosphorylation of ODAM by BMPR-IB. To investigate the special roles of ODAM phosphorylation during ALC differentiation, the selective and time-dependent induction of ODAM phosphorylation was evaluated using an immunoprecipitation assay after 14 days of ALC culture with differentiation medium. The level of ODAM phosphorylation increased from days 4 to 10, whereas it was slightly decreased between days 10 and 14 (Fig. 5A).

BMP-2 has been reported as a potent inducer of ameloblast differentiation [Coin et al., 1999]. However, the downstream molecular events and critical target genes of BMPs during amelogenesis remain unclear. It was also reported that MAPK could be regulated by TGF-β/BMP stimulation [Derynck and Zhang, 2003; Moustakas and Heldin, 2005]. To assess the effects of ODAM phosphorylation on MAPK signaling during BMP signaling, we examined the expression levels of MAPKs, including ERK, JNK, and p38/MAPK. In the presence of BMP-2, ODAM overexpression increased the phosphorylation of ERK, p38, and JNK, whereas ODAM depletion decreased ERK, p38, and JNK phosphorylation (Fig. 5B). However, the expression levels of ERK, p38, and JNK were not changed by ODAM depletion or overexpression (data not

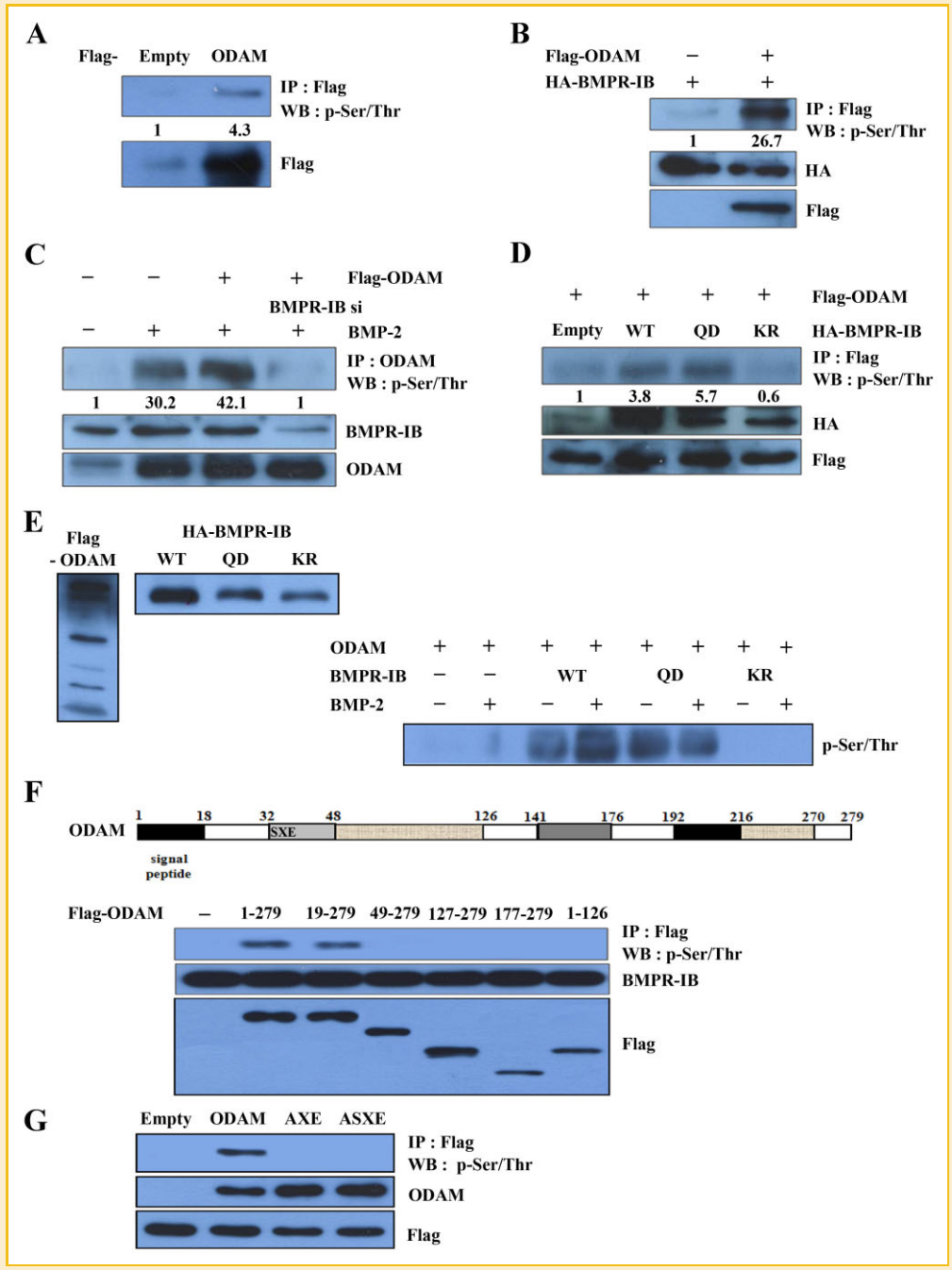

Fig. 4. ODAM phosphorylation by BMPR-IB and identification of the binding site. A,B: HEK 293 cells were transfected with Flag-tagged ODAM and/or HA-tagged BMPR-IB and treated with BMP-2 (100 ng/ml) for 16 h, and then immunoprecipitated with anti-Flag antibody. ODAM phosphorylation was evaluated by Western blotting using anti-p-Ser/Thr antibody. Densitometric quantification of ODAM phosphorylation (middle panel). C: HEK 293 cells were transfected with Flag-tagged ODAM or BMPR-IB siRNA and treated with BMP-2. Cells were immunoprecipitated with anti-ODAM antibody and protein A/G agarose and then immunoblotted with the indicated antibodies. D: HEK 293 cells were transfected with HA-tagged active BMPR-IB QD or HA-tagged inactive BMPR-IB KR together with Flag-tagged ODAM and treated with BMP-2 (100 ng/ml). E: Direct phosphorylation of ODAM by BMPR-IB. Flag-ODAM and HA-BMPR-IB were translated in vitro by TNT reticulocyte (left panel). In vitro-translated ODAM and BMPR-IB were incubated in the presence of BMP-2. BMPR-IB kinase activity was assessed and visualized by Western blotting using anti-p-Ser/Thr antibody. F: Identification of the site at which ODAM is phosphorylated by BMPR-IB. HEK 293 cells were transfected with Flag-tagged full-length ODAM or its deletion constructs and treated with BMP-2. Western blotting using anti- p-Ser/Thr antibody was performed for precipitates obtained using the anti-Flag antibody. G: Induction of phosphorylation of the ODAM SXE motif by BMPR-IB. HEK 293 cells were transfected with Flag-tagged ODAM mutants (AXE and ΔSXE). Cells were immunoprecipitated with anti-Flag antibody and protein A/G agarose and then immunoblotted with the indicated antibodies. [Color figure can be seen in the online version of this article, available at http://wileyonlinelibrary.com/journal/jcb]

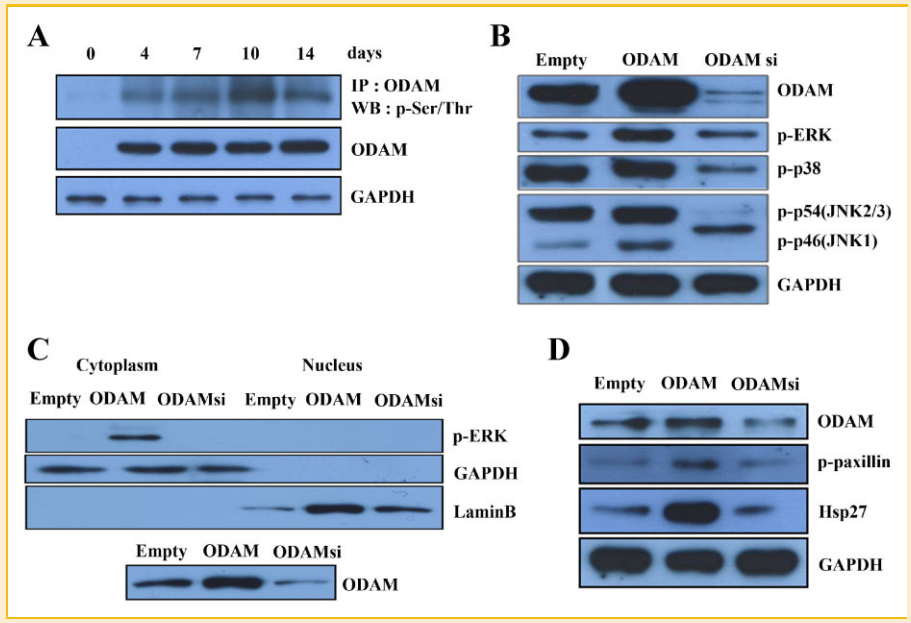

Fig. 5. Pattern of ODAM phosphorylation during ameloblast differentiation and the regulation of the downstream MAPK pathway by p-ODAM. A: Western blot analysis of the expression pattern of ODAM phosphorylation during in vitro ALC differentiation. B: ALC cells stably transfected with empty, ODAM, or ODAM-antisense expression vectors were selected by G-418 treatment. The cellular levels of p-ERK, p-p38, and p-JNK were evaluated by Western blotting after ODAM overexpression or depletion, and treatment with BMP-2. C: After ODAM overexpression or depletion, p-ERK levels in the nuclear and cytoplasmic fractions of ALC cells were evaluated by Western blotting. D: After ODAM overexpression or depletion, p-paxillin, and Hsp27 levels in ALC cells were evaluated by western blot. [Color figure can be seen in the online version of this article, available at http://wileyonlinelibrary.com/journal/jcb]

shown), implying that ODAM regulates the phosphorylation of MAPKs rather than alter their expression.

Nuclear signaling by many cellular stimuli depends on activation of the MAPK cascade and the localization of active MAPK to the nucleus, where certain enzymes can act on their target substrates. Such nuclear signaling depends on MAPK translocation from the cytoplasm to the nucleus [Lenormand et al., 1998]. To determine whether phosphorylated ERK also translocated to the nucleus, p-ERK was examined in the nuclear and cytoplasmic fractions of ODAM-overexpressed or ODAM-depleted ALC cells in the presence of BMP-2. P-ERK immunoreactivity was detected at high levels in the cytoplasmic fractions of ODAM-overexpressed ALC cells compared to the immunoreactivity in control or ODAM-depleted ALC cells (Fig. 5C). This result suggests that p-ERK, which is regulated by p-ODAM, functions primarily in the cytoplasm of ameloblasts.

p38 MAPK and tyrosine kinases are implicated in actin polymerization and contraction through heat shock protein 27 (Hsp27) and the cytoskeletal protein paxillin, respectively [Srinivasan et al., 2008]. To investigate whether phosphorylated ODAM could regulates paxillin and Hsp27 via ERK and p38 MAPK pathways, we evaluated the expression of p-paxillin and Hsp27 by Western blotting after ODAM overexpression or depletion in ALC cells. P-ODAM induced the expression of p-paxillin and Hsp27 (Fig. 5D). These data demonstrate that p-ODAM is involved in the activation of the downstream factors of ERK and p38 MAPK, paxillin and Hsp27, respectively. The findings also suggest that paxillin and Hsp27 have important roles in cytoskeleton organization in various ODAM-expressing cells including JE, ERM, and breast cancer cells.

FUNCTIONAL SIGNIFICANCE OF BMPR-IB-MEDIATED ODAM PHOSPHORYLATION IN AMELOBLASTS IN VITRO

In order to evaluate the effect of BMPR-IB on ameloblasts differentiation, we investigated the ALP activity after BMP-2 treatment or transfection with the BMPR-IB siRNA in ALC cells by ALP staining. BMP-2 treatment increased BMPR-IB activity and resulted in the increase of ALP activity in ALC cells compared to ALC cells without BMP-2, whereas the inactivation of BMPR-IB by siRNA transfection resulted in the decrease of ALP activity despite of the presence of BMP-2 (Fig. 6A).

To explore the functional significance of ODAM phosphorylation in ameloblasts, we cultured ALC cells transfected with control siRNA, BMPR-IB siRNA, ODAM construct, or ODAM SXE mutants (AXE and ΔSXE), and evaluated the formation of mineralized nodules by alizarin red-S staining. Alizarin red-S staining revealed the presence of mineralized nodules from days 10 to 14 in normal (control) ALC cells. ODAM over-expression significantly enhanced mineralized nodule formation from days 7 to 14 compared to normal cells. However, the transfection of BMPR-IB siRNA inhibited the mineralization process of ALC cells. Also, ODAM SXE mutants failed to induce the formation of mineralized nodules compared with ODAM over-expression (Fig. 6B). These data suggest that ODAM phosphorylation through BMP signaling pathway has important roles in ameloblasts differentiation and enamel mineralization.

DISCUSSION

More than 74 proteins were identified as ODAM-interacting proteins by protein microarray analysis in this study. These proteins can be

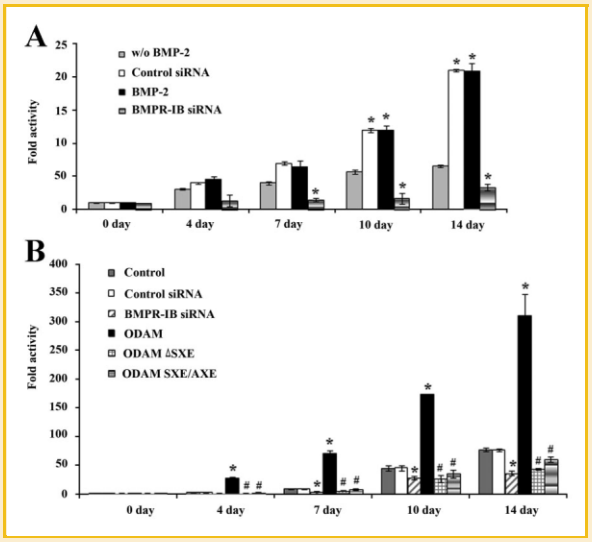

Fig. 6. Effects of BMPR-IB and ODAM on ameloblasts differentiation and enamel mineralization evaluated by ALP and alizarin red S staining. A: ALP activity was evaluated by ALP staining in BMP-2-treated or stable BMPR-IB siRNA-transfected ALC cells. ALP staining was performed at 0, 4, 7, 10, and 14 days after culture. B: ALC cells, transfected with control siRNA, BMPR-IB siRNA, ODAM construct, or ODAM SXE mutants (AXE and ΔSXE) constructs, and cultured for 14 days in differentiation medium. Cells were stained with alizarin red S at 0, 4, 7, 10, and 14 days after culture. Data are presented as mean ± standard deviation of triplicate experiments. An asterisk (*) denotes values significantly different from the control ($P < 0.05$). A number sign (#) indicated significantly comparative to the ODAM. w/o BMP-2; without BMP-2.

used as novel clues for elucidating the function of cytoplasmic ODAM in various cells. Although most of these proteins cannot explain the expanding role of ODAM, some proteins identified here are physiologically relevant, such as BMPR-IB.

During tooth development, BMPR-IB and BMPR-II appear to induce cell differentiation by BMP-2 or BMP-4 in ameloblasts and odontoblasts [Nadiri et al., 2006; Li et al., 2011]. In BMPR-IA-deficient mice, tooth development was arrested at the early bud stage, but BMPR-IB expression in these mice rescued the development of the teeth, suggesting the importance of BMPR-IB during tooth formation [Li et al., 2011]. In the present study, the interaction of ODAM and BMPR-IB increased ODAM phosphorylation in a BMP-2-dependent manner and consequently facilitated ameloblast differentiation and enamel mineralization. The BMP-2 gene has been reported to be markedly upregulated in ameloblasts at the maturation stage compared with its expression in other stages [Yamamoto et al., 2006]. BMP-2 also could accelerate or support amelogenesis at the molecular level by promoting ameloblastic marker genes induction [Miyoshi et al., 2008]. However, the mechanism by which BMP-2 alters gene expression in ameloblasts during enamel development has not yet been clarified. Therefore, our findings suggest the presence of a novel BMP-2 signaling pathway in ameloblasts that promotes ameloblast differentiation and enamel mineralization through ODAM phosphorylation by BMPR-IB.

The transduction of BMP signaling is mediated by Smads or MAPK through protein–protein and protein–DNA interactions [Canalis et al., 2003]. Although Smad4 mutant tooth germ exhibited severe defects in the patterning of the dental cusps, some mutant dental epithelial cells differentiated into ameloblasts and formed the enamel matrix in a culture with cells from Smad4fl/fl mice. This suggests that the elimination of Smad4 alone is not sufficient to block BMP signaling in the dental epithelium during early tooth development [Xu et al., 2008]. This study implies that TGF-β/BMP signaling can operate in a Smad4-independent manner during tooth and palate development albeit Smad4 occupies the central part of this signaling cascade [Massague, 1998; Derynck and Zhang, 2003]. TGF-β/BMP can activate MAPK signaling pathways involving ERK, JNK, and p38 kinases pathways [Hartsough and Mulder, 1995; Yu et al., 2002]. Phosphorylated p38, JNK, and ERK were detected in ameloblasts from the secretory to maturation stages. MAPK activators enhanced amelogenin mRNA expression [Abe et al., 2007]. MEK is upstream of ERK, and multiple ERK targets influence gene transcription and translation, cytoskeletal rearrangement, cell growth, and differentiation [Cho et al., 2008]. ERK1/2 and MEK regulate the proliferation and differentiation of the dental epithelium and odontogenic tissues [Kumamoto and Ooya, 2007]. Consistent with these reports, our results demonstrated that ODAM overexpression increased the phosphorylation of ERK, p38, and JNK after BMP-2 treatment suggesting that MAPK signaling pathway is important for amelogenesis.

ODAM expression in tumors is associated with a favorable clinical prognosis in addition to having potential diagnostic and therapeutic relevance [Kestler et al., 2011]. BMPR-IB expression also reduces the number of viable cells, increases the number of nonviable cells, and stimulates apoptotic cell death. Given the loss of BMPR-IB expression at the early stages of cancer, these data suggest that decreased BMPR-IB expression correlates with poor prognosis in breast cancer patients and leads to increased breast cancer cell proliferation in vitro. This suggests that similarly as ODAM, BMPR-IB exerts an inhibitory effect on breast cancer cells [Bokobza et al., 2009; Kestler et al., 2011]. In this regard, identification of the signaling pathway initiated by BMPR-IB-mediated ODAM phosphorylation provides important information for understanding ODAM function in various tumor cells exhibiting cytoplasmic ODAM expression.

BMP-2 or constitutively active BMPR-1B induced the migration of mesenchymal cells into collagen gels by significantly promoting the expression of an extracellular matrix protein, periostin, a known valvulogenic matrix maturation mediator. Noggin, an antagonist of BMPs, or dominant-negative BMPR-IB, on the other hand, reduced the migration of mesenchymal cell aggregates [Inai et al., 2008]. These data suggest that BMP-2 and BMP signaling induce biological processes involved in mesenchymal cell migration and periostin expression. Recent studies have demonstrated that MAPKs, including JNK, p38, and ERK, play crucial roles in cell migration [Lai et al., 2001; Xia and Karin, 2004]. JNK, for example, regulates cell migration by phosphorylating paxillin [Huang et al., 2004], DCX [Gdalyahu et al., 2004], Jun [Jiang et al., 2003], and microtubule-associated proteins [Chang et al., 2003]. Interestingly, several signaling pathways that control cell migration, including the Rac, focal adhesion kinase (FAK), and Src pathways, converge at JNK [Minden et al., 1995; Almeida et al., 2000]. Studies of p38 indicate

that this MAPK modulates cell migration by phosphorylating MAPK-activated protein kinase 2/3, which appear to be important for the directionality of migration [Werz et al., 2000]. p38 activation results in the rapid activation of Hsp27, which together with related proteins is known to affect actin organization as well as cell death, and Hsp27 activation is required for the proper maintenance of cell adhesion, as it suppresses renal epithelial cell apoptosis [de Graauw et al., 2005]. ERK governs cell movement by phosphorylating myosin light chain kinase, calpain, and FAK [Glading et al., 2004; Webb et al., 2004]. Thus, the different kinases in the MAPK family all appear capable of regulating cell migration, albeit by distinct mechanisms. Particularly significant in this context is the observation that several targets of the JNK signaling pathway are proteins involved in cell migration. Collectively, ODAM in cooperation with p38, ERK, and JNK, may form a link between the integrin cell adhesion receptors and the F-actin network, and plays important roles in cytoskeleton reorganization and cell migration [Weinberg et al., 2001].

To summarize, using protein microarray technology, we identified BMPR-IB as a novel ODAM-interacting protein and confirmed ODAM phosphorylation by BMPR-IB both in vitro and in vivo. We expect that many researchers will be able to use this list of ODAM-interacting proteins to gain new insights into how ODAM communicates with components of other signaling pathways. Our gene profiling data will facilitate new approaches for the molecular analysis of amelogenesis. Future works from our laboratory will focus on more detailed analysis of several ODAM-interacting proteins and their communication with ODAM and other diverse signaling pathways.

ACKNOWLEDGMENTS

This study was supported by a grant from the National R&D Program for Cancer Control, Ministry for Health, Welfare, and Family Affairs, Republic of Korea (No. 1020140).

REFERENCES

Abe K, Miyoshi K, Muto T, Ruspita I, Horiguchi T, Nagata T, Noma T. 2007. Establishment and characterization of rat dental epithelial derived ameloblast-lineage clones. J Biosci Bioeng 103:479–485.

Aberg T, Wozney J, Thesleff I. 1997. Expression patterns of bone morphogenetic proteins (Bmps) in the developing mouse tooth suggest roles in morphogenesis and cell differentiation. Dev Dyn 210:383–396.

Almeida EA, Ilic D, Han Q, Hauck CR, Jin F, Kawakatsu H, Schlaepfer DD, Damsky CH. 2000. Matrix survival signaling: From fibronectin via focal adhesion kinase to c-Jun NH(2)-terminal kinase. J Cell Biol 149:741–754.

Bokobza SM, Ye L, Kynaston HE, Mansel RE, Jiang WG. 2009. Reduced expression of BMPR-IB correlates with poor prognosis and increased proliferation of breast cancer cells. Cancer Genomics Proteomics 6:101–108.

Canalis E, Economides AN, Gazzerro E. 2003. Bone morphogenetic proteins, their antagonists, and the skeleton. Endocr Rev 24:218–235.

Chang L, Jones Y, Ellisman MH, Goldstein LS, Karin M. 2003. JNK1 is required for maintenance of neuronal microtubules and controls phosphorylation of microtubule-associated proteins. Dev Cell 4:521–533.

Cho KW, Cho SW, Lee JM, Lee MJ, Gang HS, Jung HS. 2008. Expression of phosphorylated forms of ERK, MEK, PTEN and PI3K in mouse oral development. Gene Expr Patterns 8:284–290.

Coin R, Haikel Y, Ruch JV. 1999. Effects of apatite, transforming growth factor beta-1, bone morphogenetic protein-2 and interleukin-7 on ameloblast differentiation in vitro. Eur J Oral Sci 107:487–495.

de Graauw M, Tijdens I, Cramer R, Corless S, Timms JF, van de Water B. 2005. Heat shock protein 27 is the major differentially phosphorylated protein involved in renal epithelial cellular stress response and controls focal adhesion organization and apoptosis. J Biol Chem 280:29885–29898.

Derynck R, Zhang YE. 2003. Smad-dependent and Smad-independent pathways in TGF-beta family signalling. Nature 425:577–584.

Fujii M, Takeda K, Imamura T, Aoki H, Sampath TK, Enomoto S, Kawabata M, Kato M, Ichijo H, Miyazono K. 1999. Roles of bone morphogenetic protein type I receptors and Smad proteins in osteoblast and chondroblast differentiation. Mol Biol Cell 10:3801–3813.

Gdalyahu A, Ghosh I, Levy T, Sapir T, Sapoznik S, Fishler Y, Azoulai D, Reiner O. 2004. DCX, a new mediator of the JNK pathway. EMBO J 23:823–832.

Glading A, Bodnar RJ, Reynolds IJ, Shiraha H, Satish L, Potter DA, Blair HC, Wells A. 2004. Epidermal growth factor activates m-calpain (calpain II), at least in part, by extracellular signal-regulated kinase-mediated phosphorylation. Mol Cell Biol 24:2499–2512.

Hardwick JC, Kodach LL, Offerhaus GJ, van den Brink GR. 2008. Bone morphogenetic protein signalling in colorectal cancer. Nat Rev Cancer 8:806–812.

Hartsough MT, Mulder KM. 1995. Transforming growth factor beta activation of p44mapk in proliferating cultures of epithelial cells. J Biol Chem 270: 7117–7124.

Hosoya A, Kim JY, Cho SW, Jung HS. 2008. BMP4 signaling regulates formation of Hertwig's epithelial root sheath during tooth root development. Cell Tissue Res 333:503–509.

Huang C, Jacobson K, Schaller MD. 2004. A role for JNK-paxillin signaling in cell migration. Cell Cycle 3:4–6.

Inai K, Norris RA, Hoffman S, Markwald RR, Sugi Y. 2008. BMP-2 induces cell migration and periostin expression during atrioventricular valvulogenesis. Dev Biol 315:383–396.

Jiang G, Giannone G, Critchley DR, Fukumoto E, Sheetz MP. 2003. Two-piconewton slip bond between fibronectin and the cytoskeleton depends on talin. Nature 424:334–337.

Kawasaki K, Weiss KM. 2003. Mineralized tissue and vertebrate evolution: The secretory calcium-binding phosphoprotein gene cluster. Proc Natl Acad Sci USA 100:4060–4065.

Kemoun P, Laurencin-Dalicieux S, Rue J, Vaysse F, Romeas A, Arzate H, Conte-Auriol F, Farges JC, Salles JP, Brunel G. 2007. Localization of STRO-1, BMP-2/-3/-7, BMP receptors and phosphorylated Smad-1 during the formation of mouse periodontium. Tissue Cell 39:257–266.

Kestler DP, Foster JS, Bruker CT, Prenshaw JW, Kennel SJ, Wall JS, Weiss DT, Solomon A. 2011. ODAM expression inhibits human breast cancer tumorigenesis. Breast Cancer (Auckl) 5:73–85.

Kumamoto H, Ooya K. 2007. Immunohistochemical detection of phosphorylated JNK, p38 MAPK, and ERK5 in ameloblastic tumors. J Oral Pathol Med 36:543–549.

Lai CF, Chaudhary L, Fausto A, Halstead LR, Ory DS, Avioli LV, Cheng SL. 2001. Erk is essential for growth, differentiation, integrin expression, and cell function in human osteoblastic cells. J Biol Chem 276:14443–14450.

Lee HK, Lee DS, Ryoo HM, Park JT, Park SJ, Bae HS, Cho MI, Park JC. 2010. The odontogenic ameloblast-associated protein (ODAM) cooperates with RUNX2 and modulates enamel mineralization via regulation of MMP-20. J Cell Biochem 111:755–767.

Lenormand P, Brondello JM, Brunet A, Pouyssegur J. 1998. Growth factor-induced p42/p44 MAPK nuclear translocation and retention requires both MAPK activation and neosynthesis of nuclear anchoring proteins. J Cell Biol 142:625–633.

Li L, Lin M, Wang Y, Cserjesi P, Chen Z, Chen Y. 2011. BmprIa is required in mesenchymal tissue and has limited redundant function with BmprIb in tooth and palate development. Dev Biol 349:451–461.

Liou GY, Zhang H, Miller EM, Seibold SA, Chen W, Gallo KA. 2010. Induced, selective proteolysis of MLK3 negatively regulates MLK3/JNK signalling. Biochem J 427:435–443.

Massague J. 1998. TGF-beta signal transduction. Annu Rev Biochem 67: 753–791.

Minden A, Lin A, Claret FX, Abo A, Karin M. 1995. Selective activation of the JNK signaling cascade and c-Jun transcriptional activity by the small GTPases Rac and Cdc42Hs. Cell 81:1147–1157.

Miyoshi K, Nagata H, Horiguchi T, Abe K, Arie Wahyudi I, Baba Y, Harada H, Noma T. 2008. BMP2-induced gene profiling in dental epithelial cell line. J Med Invest 55:216–226.

Moffatt P, Smith CE, St-Arnaud R, Nanci A. 2008. Characterization of Apin, a secreted protein highly expressed in tooth-associated epithelia. J Cell Biochem 103:941–956.

Moriguchi M, Yamada M, Miake Y, Yanagisawa T. 2011. Immunolocalization of TAK1, TAB1, and p38 in the developing rat molar. Anat Sci Int 86:69–77.

Moustakas A, Heldin CH. 2005. Non-Smad TGF-beta signals. J Cell Sci 118:3573–3584.

Nadiri A, Kuchler-Bopp S, Perrin-Schmitt F, Lesot H. 2006. Expression patterns of BMPRs in the developing mouse molar. Cell Tissue Res 324: 33–40.

Nishio C, Wazen R, Kuroda S, Moffatt P, Nanci A. 2010a. Expression pattern of odontogenic ameloblast-associated and amelotin during formation and regeneration of the junctional epithelium. Eur Cell Mater 20:393–402.

Nishio C, Wazen R, Kuroda S, Moffatt P, Nanci A. 2010b. Disruption of periodontal integrity induces expression of apin by epithelial cell rests of Malassez. J Periodontal Res 45:709–713.

Onishi T, Ishidou Y, Nagamine T, Yone K, Imamura T, Kato M, Sampath TK, ten Dijke P, Sakou T. 1998. Distinct and overlapping patterns of localization of bone morphogenetic protein (BMP) family members and a BMP type II receptor during fracture healing in rats. Bone 22:605–612.

Panchision DM, Pickel JM, Studer L, Lee SH, Turner PA, Hazel TG, McKay RD. 2001. Sequential actions of BMP receptors control neural precursor cell production and fate. Genes Dev 15:2094–2110.

Sire JY, Davit-Beal T, Delgado S, Gu X. 2007. The origin and evolution of enamel mineralization genes. Cells Tissues Organs 186:25–48.

Srinivasan R, Forman S, Quinlan RA, Ohanian J, Ohanian V. 2008. Regulation of contractility by Hsp27 and Hic-5 in rat mesenteric small arteries. Am J Physiol Heart Circ Physiol 294:H961–H969.

Vader G, Lens SM. 2008. The Aurora kinase family in cell division and cancer. Biochim Biophys Acta 1786:60–72.

Webb DJ, Donais K, Whitmore LA, Thomas SM, Turner CE, Parsons JT, Horwitz AF. 2004. FAK-Src signalling through paxillin, ERK and MLCK regulates adhesion disassembly. Nat Cell Biol 6:154–161.

Weinberg JM, Venkatachalam MA, Roeser NF, Senter RA, Nissim I. 2001. Energetic determinants of tyrosine phosphorylation of focal adhesion proteins during hypoxia/reoxygenation of kidney proximal tubules. Am J Pathol 158:2153–2164.

Werz O, Klemm J, Samuelsson B, Radmark O. 2000. 5-lipoxygenase is phosphorylated by p38 kinase-dependent MAPKAP kinases. Proc Natl Acad Sci USA 97:5261–5266.

Wieser R, Wrana JL, Massague J. 1995. GS domain mutations that constitutively activate T beta R-I, the downstream signaling component in the TGF-beta receptor complex. EMBO J 14:2199–2208.

Xia Y, Karin M. 2004. The control of cell motility and epithelial morphogenesis by Jun kinases. Trends Cell Biol 14:94–101.

Xu X, Han J, Ito Y, Bringas P Jr, Deng C, Chai Y. 2008. Ectodermal Smad4 and p38 MAPK are functionally redundant in mediating TGF-beta/BMP signaling during tooth and palate development. Dev Cell 15:322–329.

Yamamoto T, Oida S, Inage T. 2006. Gene expression and localization of insulin-like growth factors and their receptors throughout amelogenesis in rat incisors. J Histochem Cytochem 54:243–252.

Yu L, Hebert MC, Zhang YE. 2002. TGF-beta receptor-activated p38 MAP kinase mediates Smad-independent TGF-beta responses. EMBO J 21:3749–3759.